 doi:10.20944/preprints202210.0172.v2

The Dirac fermion of a monopole pair (MP) model

Samuel. P. Yuguru[1]

1. Chemistry Department, School of Natural and Physical Sciences, University of Papua New Guinea, P. O. Box 320, Waigani Campus, National Capital District 134, Papua New Guinea, Tel. : +675 326 7102; Fax. : +675 326 0369; Email address: samuel.yuguru@upng.ac.pg.

Abstract

The electron of magnetic spin −1/2 is a Dirac fermion of a complex four-component spinor field. Though this is effectively addressed by relativistic quantum field theory, an intuitive form of the fermion still remains lacking. In this novel undertaking, the fermion is examined within the boundary posed by a recently proposed MP model of a hydrogen atom into 4D space-time. Such unorthodox process somehow is able to remarkably unveil the four-component spinor of non-abelian in both Euclidean and Minkowski space-times. Supplemented by several postulates, the relativistic and non-relativistic applications of the magnetic spin property are explored from an alternative perspective. The outcomes have important implications towards an alternative interpretation of quantum electrodynamics and a probable quantum universe, where quantum mechanics and general relativity are expected to merge. Such findings could pave the paths for future pursuits of physics beyond the Standard Model and they warrant further investigations.

Keywords: Dirac fermion, magnetic spin, 4D space-time, quantum universe, Standard Model

 doi:10.20944/preprints202210.0172.v2

1. Introduction

At the fundamental level of matter, particles are described by wave-particle duality, charges and their spin property. These properties are revealed from light interactions and are pursued by the application of relativistic quantum field theory. The theory of special relativity defines lightspeed to be constant in a vacuum and the rest mass of particles as, $m = E/c^2$. By definition, the particle-like property of light waves are massless photons possessing spin 1 of neutral charge. Any differences to the spin, charge and mass-energy equivalence provide the inherent properties of the particles at the fundamental level and this is termed causality. Based on quantum field theory, particles are considered as fields permeating space at less than lightspeed, where there is a level of indetermination towards unveiling their charge and spin property, while the wave property is depended on the instrumental set-up. Such definition counteracts the deterministic viewpoint of non-relativistic Schrödinger wave function, ψ, which is extremely useful in describing precisely the probability of future events for a lone particle such as an electron in orbit of the atom [1]. First, it does not account for the spin property of the particles. Second, the ψ is classically applied to physical waves such as for the water waves. Thus, it is difficult to imagine wavy form of particles freely permeating space without interactions and this somehow collapses to a point at observation [2].

At the atomic state, the energy is radiated in discrete energy forms in infinitesimal steps of Planck's radiation, $\pm h$. Such interpretation is consistent with observations except for the resistive nature of proton decay [3]. Despite such set-back, the preferred quest is to make non-relativistic equations become relativistic due to the shared properties of both matter and light at the fundamental level as mentioned above.

Preprints (www.preprints.org) | NOT PEER-REVIEWED | Posted: 13 October 2022 doi:10.20944/preprints202210.0172.v2

Beginning with Klein-Gordon equation [4], the energy and momentum operators of Schrödinger equation,

$$\hat{E} = i\hbar\frac{\partial}{\partial t}, \qquad \hat{p} = -i\hbar\boldsymbol{\nabla}, \tag{1}$$

are adapted in the expression,

$$\left(\hbar^2\frac{\partial^2}{\partial t^2} - c^2\hbar^2\boldsymbol{\nabla}^2 + m^2c^4\right)\psi(t,\bar{x}) = 0. \tag{2}$$

Equation 2 incorporates special relativity, $E^2 = p^2c^2 + m^2c^4$ for mass-energy equivalence, $\boldsymbol{\nabla}$ is the del operator in 3D space, $\hbar$ is reduced Planck constant and i is an imaginary number, $i = \sqrt{-1}$. Only one component is considered in Equation 2 and it does not take into account the negative energy contribution from antimatter. In contrast, the Hamiltonian operator, $\widehat{H}$ of Dirac equation [5] for a free particle is,

$$\widehat{H}\psi = (-i\boldsymbol{\nabla}.\boldsymbol{\alpha} + m\beta)\psi. \tag{3}$$

The ψ has four-components of fields with vectors of momentum, $i\nabla$ and gamma matrices, $\alpha.\ \beta$ represent Pauli matrices and unitarity with m equal to particle mass. The concept is akin to, $e^+ e^- \longrightarrow 2\gamma$, where the electron annihilates with its antimatter to produce two gamma rays. Antimatter existence is observed in Stern-Gerlach experiment and positron from cosmic rays. While the relativistic rest mass is easy to grasp, how fermions acquire mass other than Higgs field remains

Preprints (www.preprints.org) | NOT PEER-REVIEWED | Posted: 13 October 2022 doi:10.20944/preprints202210.0172.v2

yet to be solved at a satisfactory level [6]. But perhaps, the most intriguing dilemma is offered by the magnetic spin ±1/2 of the electron and how this translates to a Dirac fermion of a four-component spinor. Such a case remains a very complex topic, whose intuitiveness in terms of a proper physical entity remains lacking. In this novel undertaking, the electron is examined within the boundary posed by a recently proposed MP model of 4D space-time of a hydrogen atom. With this process, the transition of the electron to a Dirac fermion is unveiled. Supplemented by a number of postulates, the fermion's relationships to both relativistic and non-relativistic aspects of the spin property are examined within the context of current knowledge. Such outcomes demonstrate the dynamics of the model, where its compatibility to a quantum universe and quantum field theory is presented. These findings if considered, could pave alternative paths for the pursuits of physics beyond the Standard Model and they warrant further investigations.

2. Dirac fermion of a MP model

An intuitive conversion of the electron to a Dirac fermion of four-component spinor field by Lorentz transformation in Euclidean space-time of non-abelian is presented in Fig. 1a. In Fig. 1b, Minkowski space-time for the fermion of spin ±1/2 in superposition states is offered. From these illustrations, a number of postulates are drawn from the first principle of space-time.

1) A lone electron within the MP model (Fig. 1a) is likened to Bohr model of the hydrogen atom. Its circular orbit is transformed to an ellipsoid of a MP field, where its precession into 4D space-time is of a clock face (Fig. 1a). The boundary is defined by an electric field, **E**. Its perpendicular dissection is assumed by quantized states of Bohr orbits (BOs) in degeneracy and these possess magnetic field, **B** (Fig. 1b) The BOs of the MP field of a

Preprints (www.preprints.org) | NOT PEER-REVIEWED | Posted: 13 October 2022 doi:10.20944/preprints202210.0172.v2

dipole moment are polarized in accordance with Pauli exclusion principle. In multielectron atoms, multiple MP fields are assumed for the electron distributions.

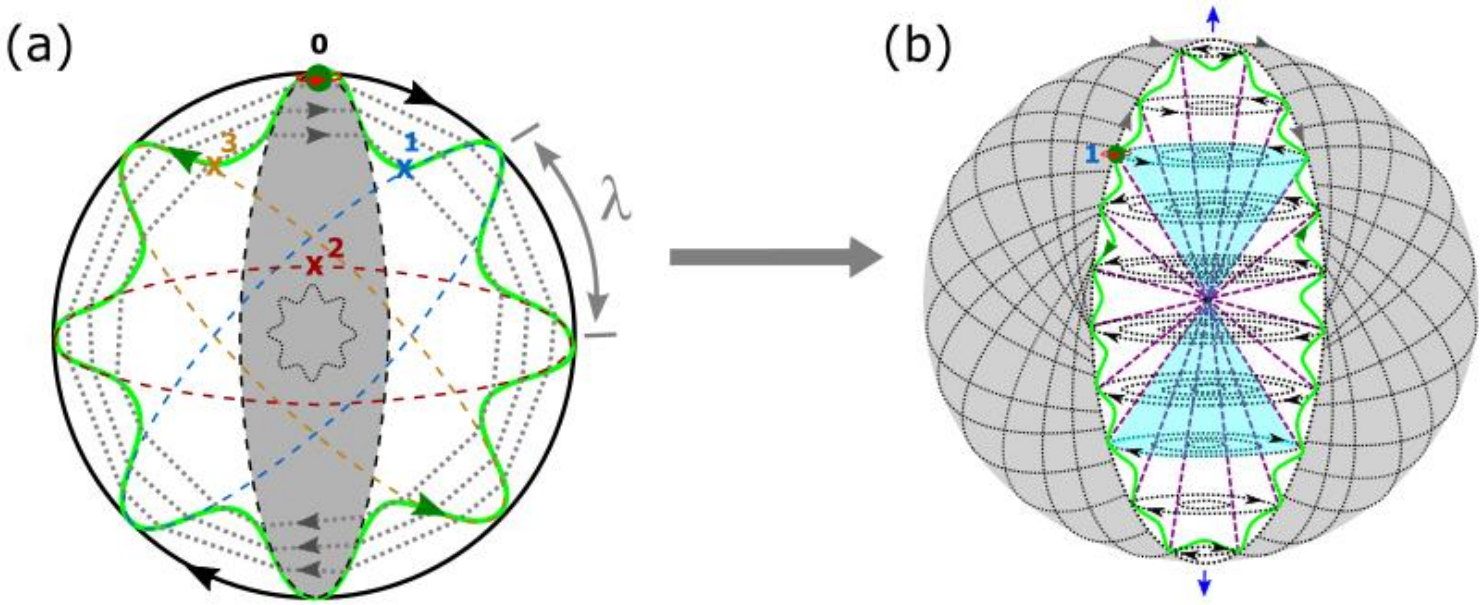

Figure 1. The MP field of an electron-wave diffraction. Image adapted from ref. [7]. (a) A spinning electron's (green dot) orbit of a circular mode is transformed to an ellipsoid MP field (grey area) and this precesses into 4D space-time of a clock face (black and grey arrows). The orbit is of time reversal due to gravity. To *an external observer*, the electron pops in and out of existence at positions, 0, 1, 2, 3 in repetitive process of a clock face by their respective colored MP fields. In this way, Schrödinger's electron field, ψ is transformed to a Dirac fermion of four-component spinor field, $i\gamma^0\gamma^1\gamma^2\gamma^3$ of spin ±1/2 in superposition states. Orthogonal projection of chirality, $\frac{1}{2}(1 \pm i\gamma^0\gamma^1\gamma^2\gamma^3)$ is reduced to the spin, $\frac{1}{2}(1 \pm i\gamma^1\gamma^3)$ at positions 1 and 3. Both are integrated into the model, where 360° rotation of the electron about positions 0, 1, 2 and 3 to 180° spherical rotation of a hemisphere generates antimatter. At 720° rotation to a 360° spherical rotation, qubits, 0 and ±1 are produced. Such twisting and unfolding process replicates both the Dirac belt trick [8] and Balinese cup trick [9]. The area defined by the shift in positions of the Dirac fermion is of non-abelian Euclidean lattice (hemisphere), whereas the sphere identifies with Euclidean space-time. (b) The MP field (white area) at position 1 is projected along the vertical axis for an

Preprints (www.preprints.org) | NOT PEER-REVIEWED | Posted: 13 October 2022 doi:10.20944/preprints202210.0172.v2

electron cloud model. Minkowski space-time is applicable to *an internal observer* positioned at the center, where the Dirac matrices, $\gamma^{1,3}$ translate to the spin property of a pair of light-cones (navy colored) in superposition states, ±1/2 at the BOs into *n*-dimension. In Hilbert space, the spin angular momentum of the orbit (purple dotted lines) is projected towards singularity at the center. Its outward projection relates to the precession of the overarching MP field. The arrow of time of a light-cone in asymmetry is unidirectional and this translates to a magnetic dipole moment (blue arrows) of the MP field. The boundary is defined by **E** and this is dissected perpendicularly along BOs (dotted loops) of **B** in degeneracy.

2) The electron's orbit of time reversal due to gravity undergoes two times rotations against the precessing MP field of a clock face into 4D space-time (Fig. 1a). The process somehow transforms the Schrödinger's electron field, ψ to a Dirac fermion of four-component spinor fields of non-abelian. The electron's transition between two points is Hermitian, $\psi \rightarrow \psi^*$ and this generates Planck's radiation, $\pm h$ with unitarity, λ sustained. h is linked to the light-cone in superposition states (i.e., ±1/2 spins) at the *n*-dimensions of BOs in degeneracy (Fig. 1b). Angular momentum, time dilation and length contraction are applicable to the light-cone for an internal observer at the center. Energy is quantized with external light interactions, i.e., $E = nhv$. The electron somehow resembles a classical object but assumes the De Broglie wave-particle duality, $\lambda = h/p$.
3) The spherical boundary of the MP model obeys the "natural units", $\hbar = c = 1$ for a local gauge field with its rotation attained in accordance with Euler's formula, $e^{i\pi} + 1 = 0$. The hemispheres offer ±1 charge of a clock face (Fig. 1a). The electron's position is defined by, $i\hbar$ in accordance with the uncertainty principle, $\Delta E.\Delta t \geq \hbar/2$ or alternatively, $\Delta x.\Delta p \geq \hbar/2$ of time invariance.

Preprints (www.preprints.org) | NOT PEER-REVIEWED | Posted: 13 October 2022 doi:10.20944/preprints202210.0172.v2

4) At 360° rotation, Dirac four-component spinor, $\psi = \begin{pmatrix} \psi_0 \\ \psi_1 \\ \psi_2 \\ \psi_3 \end{pmatrix}$ assumes their own antimatter at positions, 0, 1, 2 and 3 and matter is restored at 720° rotation (Fig. 1a). The process is attained at more than the lightspeed or complete spherical rotation of 360° for the classical qubits, 0 and 1. Stern-Gerlach experiment for the extraction of both matter and antimatter existence is applicable to the orbiting electron in 4D space-time . Only two positions ψ_1 and ψ_3 generate observable light-cones (Fig. 1b) for the intrinsic spin, ±1/2 property and are connected by a geodesic curve of a close loop mimicking the BO. The outcome of each spin is determined by Born's probabilistic interpretation,$|\psi|^2$, where the past or future paths of the electron between positions, 0, 1, 2 and 3 are not accounted for at observations. This supposes that there are no hidden variables, while a complementary photon pair interaction with the electron can be examined for the correlation of their spin property at a distance in an entanglement scenario.

5) In a multiverse of the models at a hierarchy of energy scales, the procession ensues in the following manner, nucleus => atom => planet => star => galaxy. There is obvious distinction to matter between the scales such as life on Earth and gluons at the nucleus. However, the underlying energy scale is possibly dictated by the MP model. For example, to an external observer, the shift of the Dirac fermion at positions 0, 1, 2 and 3 due to gravity of time reversal against forward time of a clock face could somehow relate to particles popping in and out of existence for the quantum state. The continuous process would indicate an exponential increase in the number of particles. At the planetary scale, this could perhaps relate to the perihelion precession of Mercury. Thus, the electron to atom is comparable to satellite to planet, planet to star and possibly star to galaxy.

Preprints (www.preprints.org) | NOT PEER-REVIEWED | Posted: 13 October 2022 doi:10.20944/preprints202210.0172.v2

6) If time of a clock face resembles the precession of the MP field into 4D space-time (Fig. 1a), it ticks slower towards the higher hierarchy of scales in a multiverse consistent with the twin paradox narrative. Thus, an observer on Earth is subject to an electron cloud model for the atom (Fig. 1a) and perihelion precession of Mercury (*Postulate 5*). The shift in the sun's precession about the Milky Way is redshifted or occurs about eight minutes slower before it is observed on Earth. Precession of the visible universe defined by the cosmic microwave background of a MP field type is microwave redshifted and its precession is then considerably redshifted to an observer on Earth in an accelerated frame of reference [7]. Such a scenario could present accelerated expansion of the universe. Thus, Clausius's conservation of energy for the universe is assumed, where entropy is recycled in a multiverse (*Postulate 5*) by the application of 2nd law of thermodynamics at reduced rate towards the higher hierarchy of scales (*Postulate 6*).
7) The non-relativistic Schrödinger ψ is assigned to the electron or its particle-hole symmetry. Its relativistic transformation to Dirac fermion within a hemisphere (Fig. 1a) is referenced to linear time in the *z* direction along positions, 0 and 2. The plane waves are projected in *x* or *y* directions at positions 1 and 3. The other hemisphere of a hologram sustains the dipole moment of the precessing MP field (Fig. 1a).

These postulates with respect to the unveiled Dirac fermion of four-component spinor field are tantamount to the tenets of physics. How these become relevant to both relativistic and non-relativistic interpretations of the electron field, ψ of the hydrogen atom are further explored in this study with some of their implications discussed. The outcomes are expected to offer new insights to existing knowledge in physics from an alternative perspective.

Preprints (www.preprints.org) | NOT PEER-REVIEWED | Posted: 13 October 2022 doi:10.20944/preprints202210.0172.v2

3. Consolidation of the model

The spin property alluded within the MP model and the offered postulates are explored for their applicability to quantum physics. First, the limitations to the applications of quantum field theory are briefly discussed. Next, the model's relevance to both quantum mechanics and relativity is elucidated by including some examples of observational scenarios. In the final section, the implications to high-energy physics, general relativity and Dirac spinor are expounded by assuming a quantum universe in a multiverse of the models at a hierarchy of energy scales.

3.1 Limitations of quantum field theories (QFTs)

QFT considers matter to be made up of fields at the fundamental level. Electromagnetism, gravity, weak and strong nuclear forces permeate these fields and are mediated by the particle types known as the bosons of 0 to ±1 charges and spin 1. Only gravity is mediated by the boson type called the graviton of spin 2. The quanta of the fields resemble particle-like property of spin 1/2 with variable charges and these are termed fermions. Light-matter (or particles) interactions induce vacuum fluctuations and polarizations, where virtual particles pop in and out of existence. The above processes are captured well by Feynman diagrams and are adapted into QFT such as quantum electrodynamics. The theory has seen a tremendous success to account for light interactions with atoms such as the splitting of hydrogen spectral lines to fine structure. However, there are two major limitations to such approach. First, a complex task of renormalization is normally done by computation to constrain the effects of particles' self-

Preprints (www.preprints.org) | NOT PEER-REVIEWED | Posted: 13 October 2022 doi:10.20944/preprints202210.0172.v2

interactions via virtual photons exchanges in order to conform to measurements. The process defeats the heuristic rule of naturalness [10] and brings into question what the approximate physical structure of matter at the fundamental level is like. Second, gravity warps the fabric of space-time based on the theory of general relativity. Its quantization as a force is yet to be defined without gravitons observed in experiments conducted so far. Other physics phenomena constrained by the application of QFTs include, neutrino mass, matter-antimatter asymmetry, dark matter, dark energy and so forth. For these reasons, the MP model offers an alternative path to the interpretation of the Dirac fermion and its spin property (Fig. 1a and b). How this relate to the electron, ψ and hence, hydrogen atom is further explored in this section.

3.2 Non-relativistic aspects of the hydrogen atom

The electron in orbit resembles the Bohr model of the hydrogen atom, whereas its translation to 4D space-time is of Dirac fermion (Fig. 1a; *Postulate 1*). Its non-relativistic Schrödinger field, ψ in 3D space is defined by the spherical polar coordinates, Ω, Φ, θ with respect to the Cartesian coordinates, x, y, z (Fig. 2). The angular component is assigned to the BO and this is defined by θ and Φ within a cylindrical boundary. The radial component into n-dimension is referenced to the z-axis. The configurations of ψ due to the precession of the MP field is defined by Ω of a von Neumann entropy state (Fig. 2). The microcanonical ensemble for the entropy, $S = k\ In\ \Omega$ is applicable to the model, with k providing an approximation of the exponential rise in the continuous shifts in the positions of the fermion along the quantized states of BOs (*Postulate 6*). The precession of the spherical model then assumes the integrals [11],

Preprints (www.preprints.org) | NOT PEER-REVIEWED | Posted: 13 October 2022 doi:10.20944/preprints202210.0172.v2

$$\int_0^{\infty}\int_0^{\pi}\int_0^{2\pi} f(r)r^2 sin\theta dr d\theta d\phi = \int_0^{\infty} f(r)4\pi r^2 dr. \quad (4)$$

where the polar coordinates for the axes are, $x = rsin\theta cos\phi$, $y = rsin\theta sin\phi$ and $z = rcos\theta$ (Fig. 2). The shift in the position of the electron during orbit is defined by $\hbar$ and it is also applicable to the Dirac fermion (Fig. 1a; *Postulate 3*). Thus, $i\hbar$ for the particle obeys the Euler's

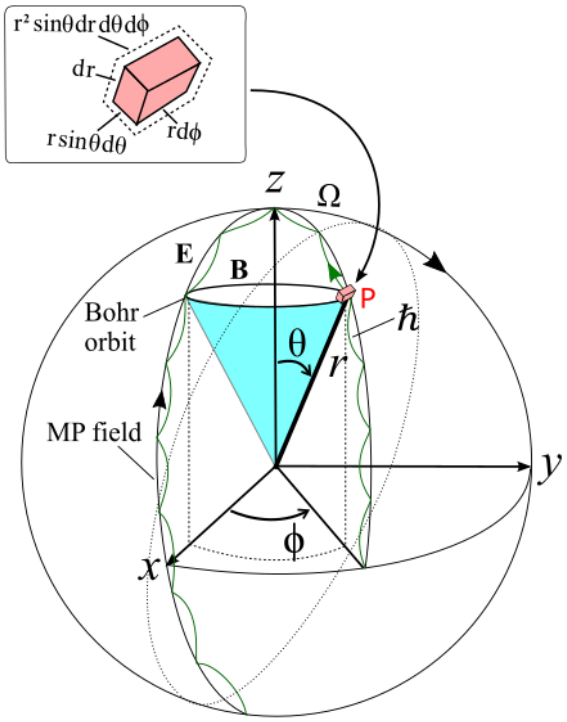

Figure 2. The electron forms the excitation of a circular standing wave (green wavy curve) of Schrödinger Ψ within the MP field (see also Fig. 1b). The polar coordinates are referenced to the center. Image modified from ref. [11].

form, $\Psi^{i\theta} = cos\theta + i\, sin\theta$. Its evolution with time adheres to the general non-linear Schrödinger's equation,

$$i\hbar\frac{\partial\psi}{\partial t}(x,t) = \hat{H}\psi\,(x,t). \quad (5)$$

The Hamiltonian operator, $\hat{H}$ is assigned to the orbital paths of unidirectional and is also applicable to Dirac fermion (Equation 3). Infinitesimal radiation of $\hbar$ is accorded to the 2nd law of thermodynamics (*Postulate 6*). Equation 5 is first order in space-time with indeterminacy in the spin property offered by the Dirac fermion in 4D space-time (Fig. 1a) and this somehow

Preprints (www.preprints.org) | NOT PEER-REVIEWED | Posted: 13 October 2022 doi:10.20944/preprints202210.0172.v2

obeys the Schrödinger cat narrative. The $\Psi_{n,l,m,ms}$ incorporates principal quantum number (n), angular momentum quantum number (l), magnetic quantum number (m) and magnetic spin (m_s). How these aligned with observations is examined next.

3.3 Relativistic transformation of the hydrogen atom

Much of the data generated for the atom or its quantum state with theoretical applications due to light-matter interactions involve relativistic interpretations. In this case, the Schrödinger electron field, ψ in Hilbert space (Fig. 1b and 2) is transformed to four-component spinor field of the Dirac fermion in Euclidean space-time within a hemisphere with an overarching hemisphere of the MP field forming a hologram (Fig. 1a). Actual measurement is reduced to 1D space of linear time as a function of traversing electromagnetic waves along straight paths. These explanations

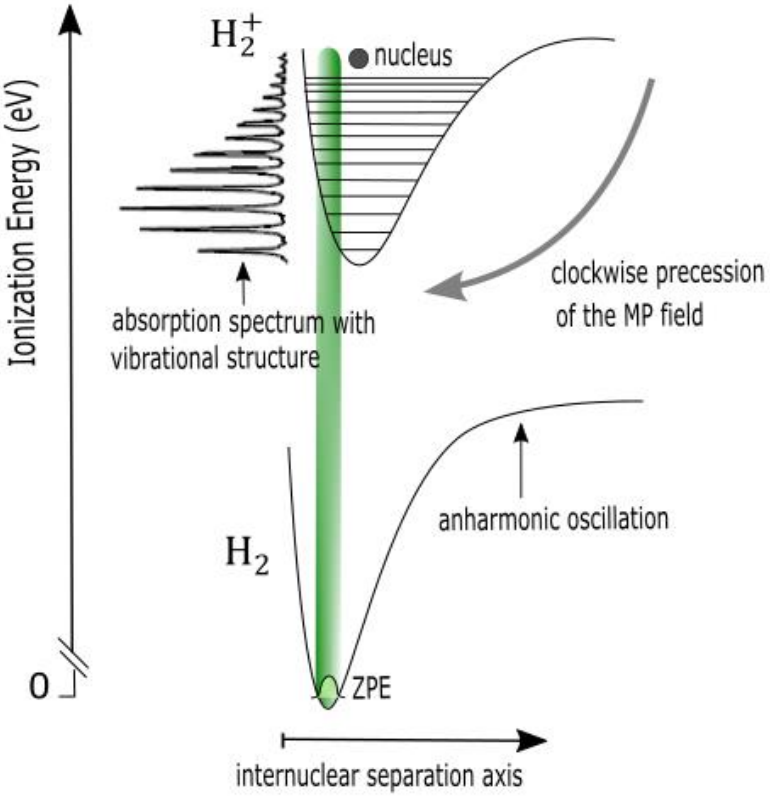

Figure 3. A schematic diagram of the photoelectron spectrum of H_2 molecule [12]. The point-boundary of the so-called zero-point energy (ZPE) at assumed at the 0 position (Fig. 1a). The shift in precession generates anharmonic oscillation. Absorption is quantized along the vibrational states of BOs.

Preprints (www.preprints.org) | NOT PEER-REVIEWED | Posted: 13 October 2022 doi:10.20944/preprints202210.0172.v2

are relatable to the hydrogen oscillator (Fig. 3), where observations at either *x* or *y* directions are referenced to the *z* direction of linear time. The fermion at positions 0 and 2 are aligned with the *z*-axis and positions 1 and 3 are interchangeable with either *x*- or *y*-axes (Fig. 1a). The BOs of a close loop offer quantized energy, $E = nhv$ for the electron's orbit with ZPE at $n = 1$ linked to position 0 (*Postulate 3*). In this way, the *n*-dimensions of the BOs incorporate the vibrational energy spectrum, $E_n = \left(n + \frac{1}{2}\right)\hbar\omega$, with ω the assumed angular frequency (Fig. 3). The antisymmetric product of one-particle solutions [13] of the Dirac fermion is,

$$\psi(x_1, x_3) = \varphi_1(x_1)\varphi_3(x_3) - \varphi_1(x_3)\varphi_3(x_1)\,. \tag{6a}$$

$$\hat{P}\psi(x_1, x_3) = \varphi_1(x_3)\varphi_3(x_1) - \varphi_1(x_1)\varphi_3(x_3),$$

$$= -\psi(x_1, x_3). \tag{6b}$$

$\hat{p}$ is the probability operator for the Hermitian of the spin 1/2 property at positions 1 and 3 (Fig. 1a). φ is the spinor generated along the BOs into *n*-dimensions of Hilbert space either in outward direction from the precessing MP field or inward direction from the electron's orbit of time reversal. Both are encased by the configurations, Ω of same magnitudes (Fig. 1a and 2). These interpretations are applicable to the determination of the fine structures of the hydrogen spectral lines (Fig. 4a−d). Fourier transform is projected in either *x* or *y* directions with reference to *z* direction or intranuclear axis within the atom (Fig. 4a). A hologram sustains unitarity for the dipole moment of the MP field (Fig. 4b). Lorentz transformation of the electron-wave diffraction (Fig. 4c) induces Dirac fermion (Fig. 1a) of an oscillation mode (Fig. 4d) comparable to Fig. 3.

Preprints (www.preprints.org) | NOT PEER-REVIEWED | Posted: 13 October 2022 doi:10.20944/preprints202210.0172.v2

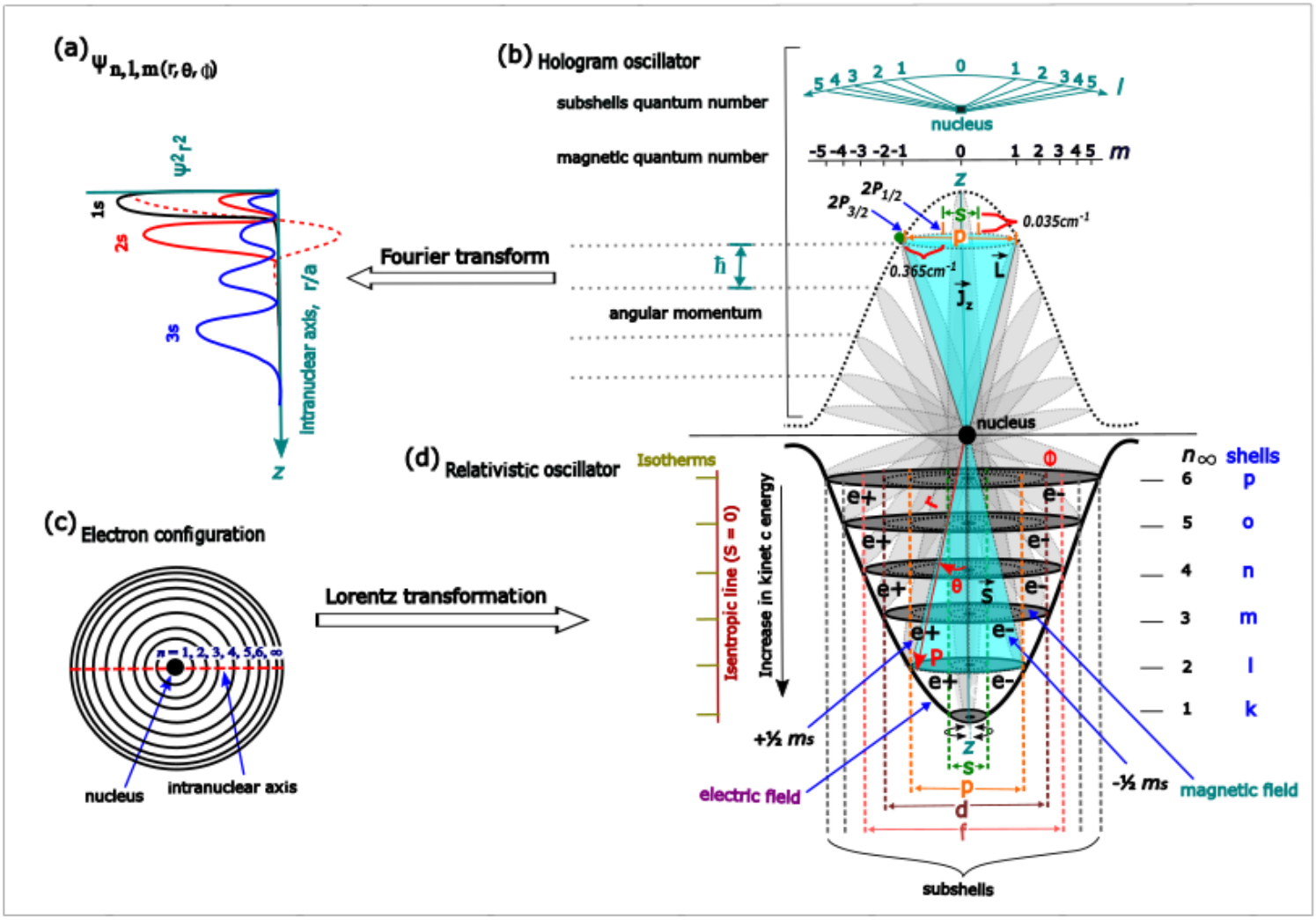

Figure 4. The MP model of the hydrogen atom. (a) Polarization of spin-orbit coupling is referenced to the vertical axis as intranuclear or *z*-axis of linear time. By Fourier transform in 1D space, both radial probability distributions, ψ_{nl} (un-dotted lines) and angular function, ψ_{lm}(red dotted line) for selected orbitals (e.g., 2*s*-orbital) are shown in either *x* or *y* directions. (b) A hologram oscillator incorporates both the 3D Schrödinger terms of reference and Dirac theory for spin-orbit splitting [14], i.e., $2P_{3/2}$ and $2P_{1/2}$ at 0.365 cm^{-1} and the lamb shift for $2P_{1/2}$ and $2S_{1/2}$ at 0.035 cm^{-1}. These are applicable to the lone electron (green dot) at position 1 (Fig. 1b), where the transition in its orbit of 4D space-time is defined by $\hbar$ (Fig. 2). (c) Electron configuration mimicking the electron-wave diffraction and its interaction with light paths energizes the *n*-dimensions of the hydrogen atom. (d) Lorentz transformation for spin-orbit coupling is

Preprints (www.preprints.org) | NOT PEER-REVIEWED | Posted: 13 October 2022 doi:10.20944/preprints202210.0172.v2

projected to either *x* or *y* directions with reference to *z* direction in general agreement to the interpretation of Dirac fermion offered by the model (Fig. 1a and b), and non-commutation, $e^+ \neq e^-$ is applicable to the BOs into *n*-dimensions in violation of lightspeed. The harmonic oscillator is assigned to a classical hemisphere (*Postulate 7*). Cooling and stabilization by external magnetic field generates an isothermal state at the *n*-dimensions. The symbols, *p*, *r*, θ and Φ (red colored) are referenced to Fig. 2.

How such interpretation translates to a double slit experimentation for entanglement without invoking hidden variables or many-worlds interpretation is offered in Fig. 5. The lone electron

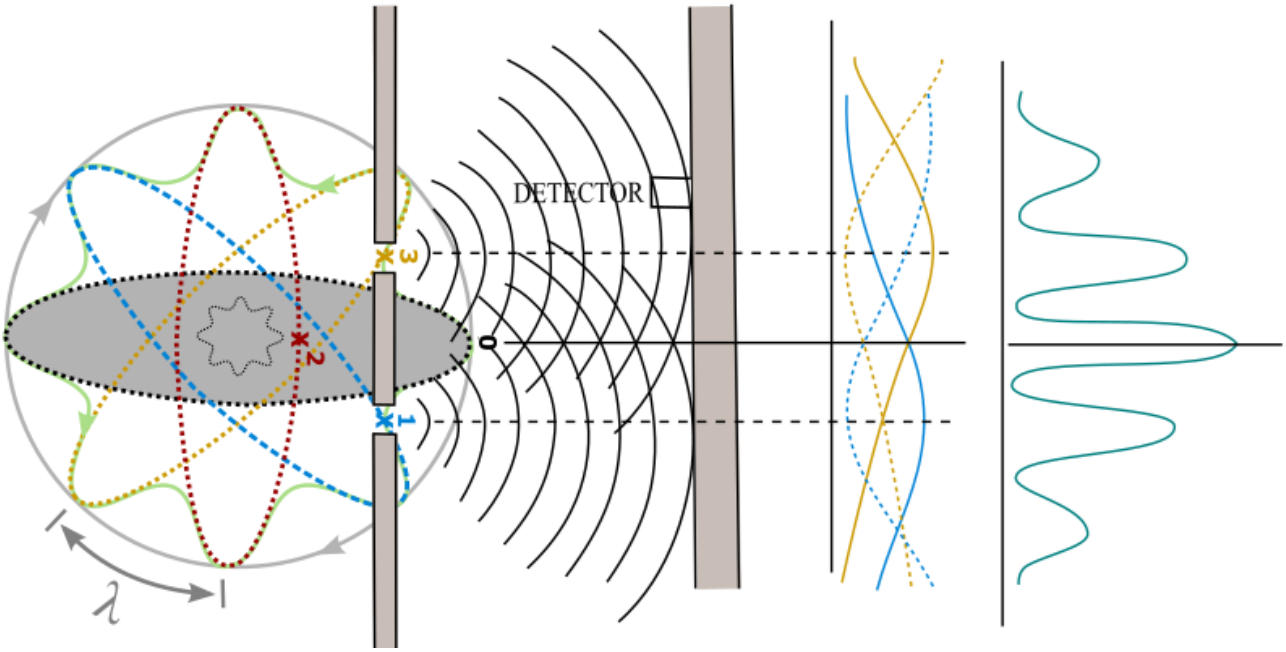

Figure 5. Wave-particle duality of Dirac fermion. The fermion (Fig. 1a) and its wave property are relatable to the double slit experiment for Born's probabilistic interpretation, $|\psi|^2$ by decoherence at observation (*Postulate 4*). The superposition of ±1/2 spins at positions 1 and 3 are shown by their respective colored wave functions by assuming that when the wave diffraction propagates at 360° rotation, the electron undergoes two times rotations (Fig. 1a). Observation is deterministic in 1D space (green wavy curve) comparable to Fourier transform (Fig. 4a). These interpretations are consistent with the Schrödinger's cat narrative and hence, the wave function collapse scenario.

Preprints (www.preprints.org) | NOT PEER-REVIEWED | Posted: 13 October 2022 doi:10.20944/preprints202210.0172.v2

in its orbit attains both matter and antimatter features at 720° rotation compared to overall spherical rotation at 360° (*Postulate 4*). In 4D space-time, the electron's orbit of a monopole field is attained within a hemisphere for a spin 1/2 of either negative or positive charge (Fig. 1a). From ZPE or vacuum energy at 0 position (Fig. 1a), the transition from n = 1 to n = 2 accommodates both Dirac spinor and hence, lamb shift for the BOs in degeneracy (Fig. 4b). These are applicable to the conventional interpretation, where total angular momentum, $\vec{J} = l \pm \frac{1}{2}$, provides the values, $\frac{3}{2}$ and $\frac{1}{2}$ for n = 2, l = 1 (Fig. 6a and b). Supposing that each subshell of an

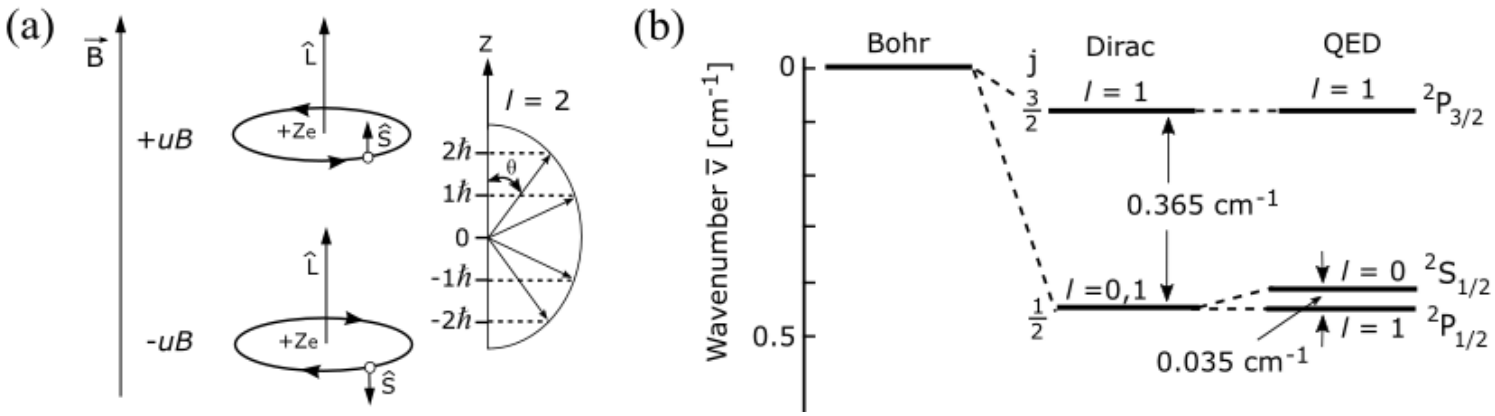

Figure 6. Spin-orbit coupling [11, 14]. (a) In the presence of a weak external magnetic field, $\vec{B}$, its dipole moment, *uB* of classical Bohr magneton exerts corresponding response from the electron's dipole moment. The spin-orbit coupling is aligned parallel to $\vec{B}$. The combined dipole is, $u_z = u_B + u_l$, with u_l equal to $\vec{J}$ and $\vec{J} = l + 1/2$. (b) When n = 2, l = 1 under unfavorable condition, $2P_{3/2}$ is produced at high energy. In the anticoupling process with $\hat{S}$ in the opposite direction, $2P_{1/2}$ is attained at a low energy. The lamb shift shows that $2S_{1/2}$ is generated probably due to the peak at n = 1 (e.g., Fig. 4d).

Preprints (www.preprints.org) | NOT PEER-REVIEWED | Posted: 13 October 2022 doi:10.20944/preprints202210.0172.v2

eigenstate possesses spin 1/2 of a light-cone (Fig. 4d), then $n_2 + n_1 = \frac{3}{2}$ (i.e., 1/2 + 1/2 + 1/2 from the combinations of *s*-*p* subshells for the electron configuration with 1s2s2p assigned to an oscillator of a monopole field). Similarly, $n_2 - n_1 = \frac{1}{2}$ for the *p* subshell is comparable to, 1/2 + 1/2 − 1/2. Due to the peak (Fig. 4b), the *s* subshell attains a slightly higher potential energy than *p* subshell at *n* = 2 (Fig. 6b). The multiplicity of the subshells, i.e., $2\left(S_{\frac{1}{2}},\ P_{\frac{1}{2}}\right)$ somehow relates to the 720° rotation before the Dirac fermion assumes its original state. Precession of the MP field allows for changes in *l* and the orientation of the *p* subshells with respect to *m* values (Fig. 4b), while the dipole moment obeys Pauli exclusion principle for the electron distribution (e.g., $1s^2 2s^2 2p^6$). These interpretations are applicable to the Clebsch−Gordon series for the total orbital angular moment, $\vec{L} = \sqrt{l(l+1)}\hbar$ and total spin, $\vec{S} = \sqrt{s(s+1)}\hbar$ at the *n*-dimensions (e.g., Fig. 6a). The lamb shift refines the value of the fine-structure constant, α to about less than 1 part in a billion [15] and this quantifies the gap between the fine structure of the hydrogen spectral lines with respect to degenerate BOs. It is an indication of the strength of the electromagnetic interaction between elementary charged particles by the relationship,

$$a = \frac{e^2}{4\pi\epsilon_0}, \tag{7}$$

where ε_0 is the vacuum permittivity and *e* is electron charge. In high-energy physics, a nondimensional system is used with the boundary, ϵ_0= c = $\hbar$ = 1, so Equation 7 becomes,

$$a = \frac{e^2}{\hbar c} \approx \frac{1}{137.036}. \tag{8}$$

Preprints (www.preprints.org) | NOT PEER-REVIEWED | Posted: 13 October 2022 doi:10.20944/preprints202210.0172.v2

No two electrons are present in the hydrogen atom so e^2 relates to the ability of the electron to undergo 720° to form both matter and antimatter, while its transition in orbit of Hilbert space into *n*-dimensions is quantized, $\hbar$ (Fig. 2). The anomalous dipole moment of the electron with respect to its *g*-factor is computed by perturbative expansion to the powers of α in the form,

$$g_e = 2\left(1 + \frac{a}{2\pi} + \cdots\right). \tag{9}$$

Equation 9 simply describes the 720° rotation for the electron as twice the classical spherical rotation at 360° in Hilbert space (Fig. 1a and b). The exponential expansion is related to continual rotation of the electron in orbit. At the present stage, the predicted and measured *g*-factor for the electron is well in agreement to about 10 decimal points [16]. The relationship between the generated magnetic moment, u_s and *g*-factor is,

$$u_s = g_e \frac{u_B}{\hbar} s, \tag{10}$$

where *s* is the intrinsic spin property of the electron. The electron is a classical Bohr magneton, u_B (Fig. 6), where its path is quantized, $\hbar$ (Fig. 2). Unlike a rotating classical object, its spin and intrinsic angular momentum are applicable in Minkowski space-time (Fig. 1b). Thus, by default, the constants, *e*, *c*, *h* and ε_o are naturally integrated into the MP model. Other related themes that can also be pursued perhaps in a similar process include Zeeman effect, quantum Hall effect, Coulomb interactions, Rydberg constant and so forth. In the subsequent section, the implications

Preprints (www.preprints.org) | NOT PEER-REVIEWED | Posted: 13 October 2022 doi:10.20944/preprints202210.0172.v2

of these presentations to high-energy physics, general relativity, Dirac spinor and its field theory are briefly examined in order to pave their future research paths from an alternative perspective.

4. The implications

The demonstrations of Dirac fermion and lamb shift in the preceding sections pose a new perspective to the nature of spin-orbit coupling in an atom. Aided by the postulates, the model offers the avenue to explore the possible relationship between quantum mechanics and general relativity from alternative standpoint. This is complemented by an intuitive demonstration of the Dirac spinor and its field theory.

4.1 Quantum universe

The Lagrangian of the Standard Model (SM) theory dealing with quantum mechanics employs quartic self-interacting term for the scalar field, Φ of particles such as the Higgs boson. Fine-tuning by the property asymptotic freedom sets the limit for the proton mass in terms of quarks in hadrons collisions [17]. The attempt to apply the same property to the electroweak force for the predicted decay of the Higgs boson is known as technicolor [18]. It requires the Planck's mass to be reduced by several orders of magnitude to the observed Higgs mass and somehow this contradicts with naturalness [19]. The problem could be solved with supersymmetry partners [20] but these are yet to be unveiled in high energy experiments such as the CERN's Large Hadron Collider [21, 22]. Unequivocally, this raises the critical question of whether the SM of

Preprints (www.preprints.org) | NOT PEER-REVIEWED | Posted: 13 October 2022 doi:10.20944/preprints202210.0172.v2

the Yang-Mills theory is complete. Similarly, to extend the SM to quantize gravity is still pending without the observations of gravitons yet to be established in experiments. Here, a quantum universe is speculated in a multiverse of the MP models at a hierarchy of energy scales. How this become relevant to the intuitive interpretations of both the SM and general relativity terms is examined.

4.1.1 The vacuum dynamics of a MP model

The electron is a Dirac fermion in its orbit and it assumes its own antimatter at 360° rotation and matter at 720° rotation of a clock face within a classical spherical rotation of 360° in Euclidean space-time (Fig. 1a; *Postulate 4*). In hadrons collisions processes, antimatter is simulated to be of time reversal, whereas in actual case, this equates to maximum twist at 360° before the unfolding process is resumed towards 720° rotation akin to both the Dirac belt trick [8] and Balinese cup trick [9]. With unitarity sustained, the electron removal by ionization is expected to generate particle-hole symmetry for the model. The vacuum or ZPE excitation of Higgs boson would then mimic the electron. In this case, both vertex corrections and Dirac annihilation process for the spin-orbit coupling are applicable to the model (Fig. 7a). Thus, if Higgs is a heavier version of the Dirac fermion at high energies (> 1 TeV), its four-component spinor field of, $H°$ and $Z°$ would translate to ψ^0 and ψ^2 at positions 0 and 2 respectively. $W^{\pm}$ bosons of doublet weak isospin of $SU(2)$ gauge symmetry for ψ^1 and ψ^3 is assumed at positions 1 and 3. The continuity of the Higgs sector at the boundary of the model of a spherical gauge field is applicable to heavy Nambu-Goldstone modes [23] of spontaneous symmetry breaking. Whether these explanations are applicable to the simulation of the Higgs excitation by controlled Raman pulses on non-

Preprints (www.preprints.org) | NOT PEER-REVIEWED | Posted: 13 October 2022 doi:10.20944/preprints202210.0172.v2

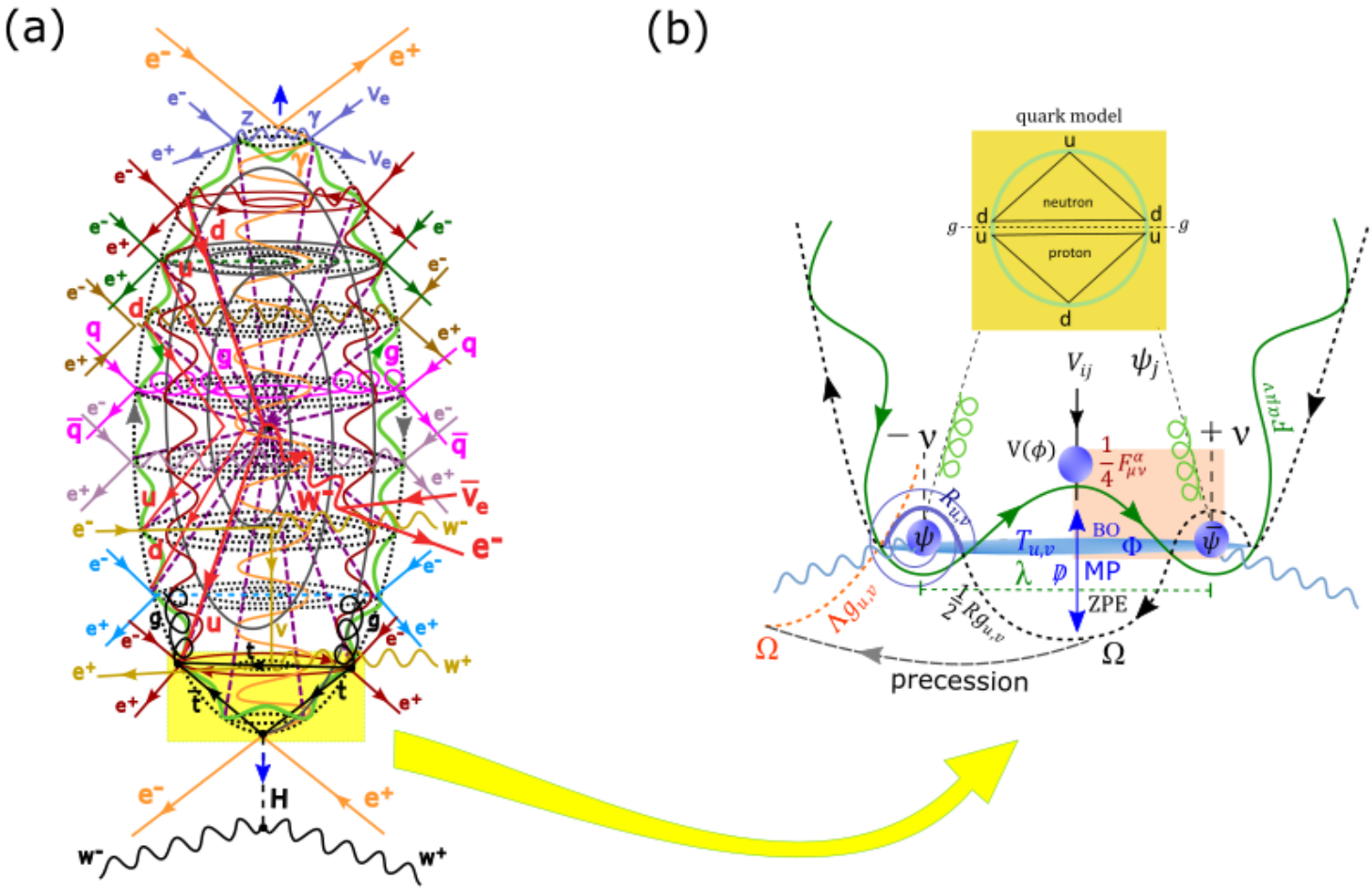

Figure 7. A quantum universe. (a) Quantum foam of vacuum fluctuations. At disturbance, a plethora of particle types is expected at the quantized states of the BOs. The process is analogous to particles popping in and out of existence in accordance with Feynman path integrals. (b) Expansion of the area highlighted in yellow is explored for the Higgs sector. The emergence of the Higgs field of ZPE is somehow related to the electron. The Dirac fermion of four-component spinor (Fig. 1a) is assumed by the Higgs boson (position 0), $W^{\pm}$ bosons (positions 1 and 3) and Z boson (position 2) of time invariant. Observation sustains $\Delta E.\Delta t \geq \hbar/2$ (*Postulate 3*) in accordance with asymptotic freedom (area highlighted in orange). Somehow, this is applicable to free reign of quark in confinement (insert image) within a hemisphere of spin 1/2. So that position 0 is occupied by the up quark and position 2 by down quark. At

Preprints (www.preprints.org) | NOT PEER-REVIEWED | Posted: 13 October 2022 doi:10.20944/preprints202210.0172.v2

positions 1 and 3, the quark is in superposition states of weak isospin and is held together by gluons. In this way, both Einstein's terms of general relativity in Euclidean space-time [7] and lagrangian mechanics [24] are intuitively applied to a quantum universe of 4D space-time. See text for brief explanations.

interacting cold hydrogenic atom (e.g., Lithium) of spin-orbit coupling in condensed physics [25] for the Higgs sector (Fig. 7b) is open to further discussions. The stability of the Higgs field is sustained by the overarching monopole field of a hologram (Fig. 4b), where the dipole moment is preserved (Fig. 7b). In this way, any decaying processes of the Higgs bosons or observations of monopoles become fairly constrained.

Suppose the nucleus resembles the MP model at the subatomic scale, a proton would indicate a triangulated pair of the quark transition at positions 0 to 3 in a superfluid state due to confinement. In this way, the quark assumes the four-component Dirac fermion in Euclidean space-time at high energy with superposition states of spin ±1/2 for up or down quark applicable to ψ^1 and ψ^3 at positions 1 and 3 (Fig. 1a; *Postulate 4*). This would translate to the proposed quark model within a hemisphere, whereby both proton and neutron are held together by gluons (Fig. 7b). Such a scenario accommodates non-abelian lattice space for *SU*(3) gauge symmetry interpretation within the SM. Thus, if the nucleon is unstable, subjecting it to electroweak nuclear decay like beta decay, $n^{\circ} \rightarrow p + W^{-} \rightarrow uud + e^{-} + \bar{\nu}$, reinforces the shown quark model with the release of antineutrino (Fig. 7b).

If the neutron dictates the next triangulated pair in the bottom hemisphere comparable to the proton, then the top and bottom quark could be incorporated at positions 0 and 2, while charm and strange quarks are linked to the superposition states at positions 1 and 3. So to access the top quark would require high energy level, while the overall spherical precession is expected to produce color change of charges with mass acquisition attained by oscillation process. Similarly,

Preprints (www.preprints.org) | NOT PEER-REVIEWED | Posted: 13 October 2022 doi:10.20944/preprints202210.0172.v2

the Dirac fermion translations to muon and tau fermions at different energy levels also remain a possibility. In this way, both hadrons and leptons can be computed at different energy scales within the MP model. The bosons should appear to be a reflection of how the model interacts with the applied external light. Translation of the overall spherical rotation of 360° would sustain linear electromagnetic radiation of $U(1)$ gauge symmetry. Such a possibility provides a way to incorporate general relativity from an alternative perspective and this is explored next.

4.1.2 Space-time curvature at the fundamental level

The idea that curved space-time could be fundamental to nature for both matter and the astrophysical universe was first proposed by assuming the existence of an object called geon (gravitational−electromagnetic entity) [26]. The geon concentrates energy and dictates the curvature of space, whereas space tells it how to move analogous to a cosmic black hole. The discrepancy to such novelty is that geon is considered to be a field and by quantum fluctuations of a quantum foamy layer, it is subject to Hawking radiations, where information is lost through time. Such a path can be reconciled with the observation of gravitons but experiments mimicking the Big Bang such as the CERN's large hadrons collider are yet to unveil them. So we are caught somehow in the middle of time trying to decipher what space-time is actually like either at the initial Big Bang scenario or to glimpse it properly from the overall expansion of the universe. Hence, a refined version of Wheeler's coinage, matter tells space-time how to curve and space-time tells matter how to move to be made fundamental evades conventional methods.

The MP model adapts Dalton's idea of atomism, where the electron is a classical object that is transformed to a Dirac fermion in an atomic universe (Fig. 1a). Such interpretation is

Preprints (www.preprints.org) | NOT PEER-REVIEWED | Posted: 13 October 2022 doi:10.20944/preprints202210.0172.v2

consistent with both Schrödinger's ψ and its relativistic transformations for the fine structures of the hydrogen atom (subsections 3.2 and 3.3). Likewise, the Hermitian of the fermion on the surface of a sphere is linked by a geodesic distance of a close loop of BO and these are relevant to Born's probabilistic interpretation of the spin property (*Postulate 4*). Thus, in a quantum universe of a multiverse of the MP models at a hierarchy of scales, Einstein's field terms of space-time geometry [27] can be differentiated from the Lagrangian terms of the SM [24] (Fig. 7b) based on the definition of the Dirac fermion in both Euclidean and Minkowski space-times of Lorentz invariance (Fig. 1a and b). Such a proposition has been made elsewhere for an object field, ψ [7]. In this case, the field tensor, $F_{u,v}$ defines the curvature of the gauge electromagnetic field. Comparably, $R_{u,v}$ is the Ricci curvature tensor of precessing MP field of a clock face induced by the presence of matter. $G_{u,v}$ is a metric tensor of 4D space-time and is linked to the *n*-dimensions. It can either contract, $\frac{1}{2}Rg_{u,v}$by gravity or expand, $\Lambda g_{u,v}$ due to precession. The stress-energy tensor, $T_{u,v}$ and Dirac notation, $\not{D}$ are incorporated by the BOs into *n*-dimensions (Fig. 1a). Yukawa coupling, V_{ij} connects the quark model to the Higgs sector (Fig. 7b). Such explanations describe the space-time geometry offered by the MP model, where Newtonian gravity is possibly localized in a universe. Its interconnectivity with others in a multiverse at a hierarchy of scales is provided by the magnetic dipole moment. In this case, the Hermitian, $\psi\bar{\psi}$ for the Higgs sector (Fig. 7b) could relate to gravitational waves emanating from the merging of binary black holes [28] if the Higgs boson appears at singularity of the gauge field defined by the model. Such a notion remains plausible when observation is confined to a portion of the Higgs sector of Lorentz invariance and is limited by the uncertainty principle, $\Delta E.\Delta t \geq \hbar/2$ (e.g., Fig. 7b; *Postulate 3*). Accelerated expansion of the universe then would mimic precession [7], where time is considerably slowed at the cosmic scale (*Postulate 7*). Observation by constant lightspeed

Preprints (www.preprints.org) | NOT PEER-REVIEWED | Posted: 13 October 2022 doi:10.20944/preprints202210.0172.v2

in a vacuum of linear time is further redshifted. All these explanations could perhaps become relevant to the alternative interpretations of the Big Bang, hierarchy dilemma, neutrino oscillations, quantum gravity, baryon asymmetry, dark matter, dark energy and so forth and they warrant further investigations.

4.2 Quantum Electrodynamics

The MP model of a dipole moment and the emergence of the Higgs amplitude (Fig. 7b) constraints the observations of monopoles as also noted in current experimental undertakings. With this process, both non-relativistic and relativistic aspects of QFT are incorporated into the model. How this becomes relevant to Dirac spinor and its field theory is further explored in this section.

4.2.1 Dirac spinor

Diagonal coupling of rotating BOs and $\vec{L}$ produces intrinsic properties of $\vec{J}$ or the spinor in units of $\hbar$ (Fig. 6a). This is applicable to the reduction of Dirac fermion of four-component spinor field to spin ±1/2 states (Fig. 1a and b). The pair of light-cones are of time invariant to the helicity of the model. The left-handed helicity is equal to 360° rotation of the fermion or positron between positions, 0 to 3, when the direction of the spin is opposite to direction of motion. This is attained within a hemisphere or equivalent to 180° rotation of the overarching spherical model (Fig. 8). Positive or right-handed helicity is restored at 720° rotation for the fermion or

Preprints (www.preprints.org) | NOT PEER-REVIEWED | Posted: 13 October 2022 doi:10.20944/preprints202210.0172.v2

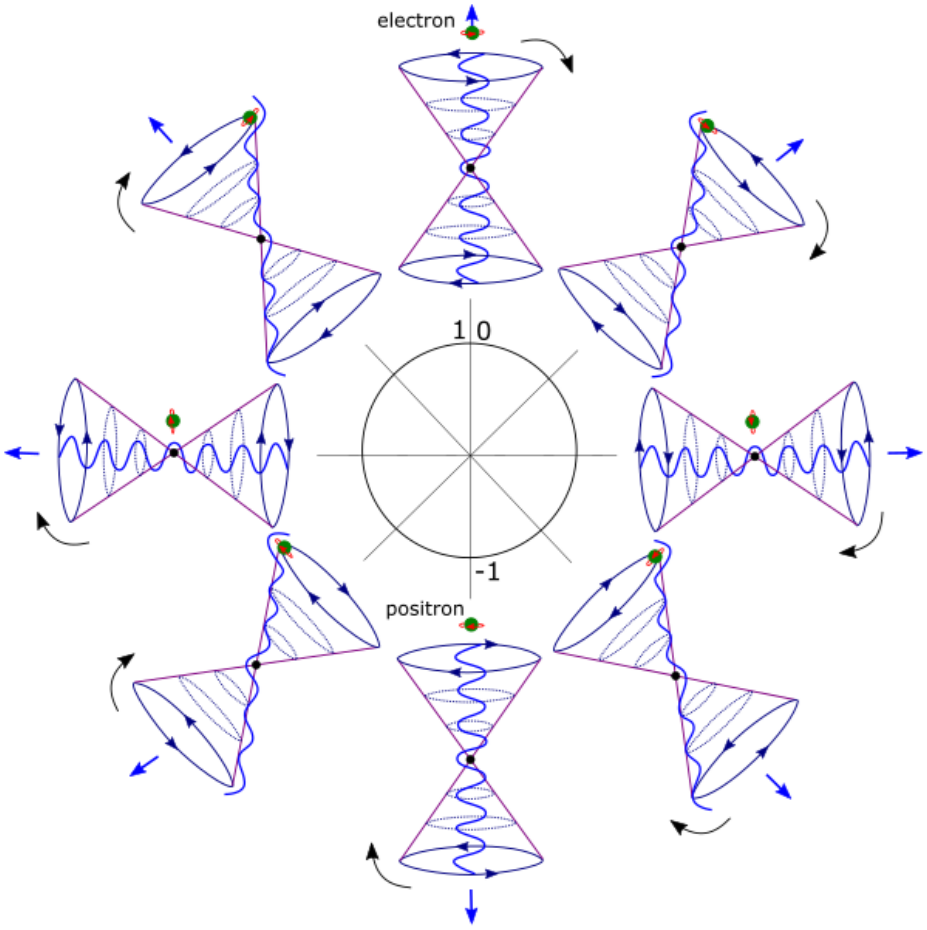

Figure 8. Dirac spinor. The transition of the Dirac fermion in Euclidean space-time (Fig. 1a) to Minkowski space-time (Fig. 1b) is explored for the spin property. The spinor (blue arrows) shows the orientation of the BOs of the light-cones at precession. At 180° spherical rotation of the electron (green dot), spin, +1/2 of negative helicity or −1 qubit is attained, where the direction of spin is opposed to direction of motion. The recoiling (blue wavy curve) of BOs from the unfolding at maximum twist repeats the rotation process to 720° or equivalent to 360° spherical rotation (i.e., qubit 1), where the electron resumes its original state of spin, −1/2 of positive helicity. Similarly, both parity transformation and chirality are also applicable to the quantized electron's orbit.

Preprints (www.preprints.org) | NOT PEER-REVIEWED | Posted: 13 October 2022 doi:10.20944/preprints202210.0172.v2

equivalent to 360° spherical rotation, where the electron resumes its original state. The process somehow indicates space inversion or parity transformation of the model through the center from 1 to −1 (Fig. 8). In this way, chiral symmetry is offered by the fermion within a hemisphere, where the four-component spinor of the Dirac fermion is of unidirectional for the spherical rotation at 360° (Fig. 1a and 8). With these interpretations, it is also possible to distinguish between Dirac, Weyl and Majorana fermions and possibly neutrinos. For example, Weyl fermion is assigned to the pair of light-cones of time invariance (Fig. 1b and 8). Each position at 0, 1, 2 and 3 (Fig. 1a) assumes its own antimatter during the twisting and unfolding process towards 720° rotation compared to 360° rotation at lightspeed and this identify with Majorana fermion. The electron itself is a Dirac fermion of four-component spinor field, while the neutrinos are possibly vibrational manifestations of the fermion. For the broad spectrum of the electromagnetic waves, the classical qubits, 0, −1 and 1 are generated but 0 and 1 dominate (Fig. 8). By combining these explanations with those offered in the previous section, the possible path for the unification of $U(1)$ x $SU(2)$ symmetry of non-abelian for the electroweak force is unveiled.

4.2.2 Dirac field theory

The theory is very well developed within the area of quantum electrodynamics with numerous literatures available. In here, certain aspects of the field theory are considered with respect to the intuitive form of the Dirac fermion unveiled in this study (Fig. 1a). Such undertaking is based on a number of selected references [29–31].

Preprints (www.preprints.org) | NOT PEER-REVIEWED | Posted: 13 October 2022 doi:10.20944/preprints202210.0172.v2

⇒ **Maxwell electromagnetism.** The spherical MP model sustains unitarity, $U(1)$ symmetry (Fig. 1b), while measurement is of linear time in 1D space. Both are applicable to the classical Maxwell's equation to describe the electron in orbit of the general form,

$$\boldsymbol{\nabla} . \boldsymbol{E}\,(\psi) = -\frac{\partial \boldsymbol{B}}{\partial t}(\psi) = m_j \hbar\,(\psi), \tag{11}$$

where $\boldsymbol{\nabla}$ is the divergence of the dipole moment of the MP field during precession and m_j is the spin momentum. **E** and **B** are orthogonal to each other in space-time (*Postulate 1*) with **B** defined by the BOs in degeneracy. The shift in the electron's position about the BO is given by the Faraday's relationship,

$$\boldsymbol{\nabla} . \boldsymbol{B}\,(\psi) = U_0 J + U_0 \varepsilon_0 \frac{\partial \boldsymbol{E}}{\partial t}(\psi), \tag{12a}$$

so that,

$$\boldsymbol{\nabla} . \boldsymbol{E}\,(\psi) = \frac{\rho}{\varepsilon_0}(\psi). \tag{12b}$$

The density, ρ of the vacuum state (Fig. 7a) is constrained to Ω of spherical configurations, whereas Ω x Ω^* is Hermitian of discrete space-time given by, $\hbar$ (Fig. 7b). The electron's orbit and its transformation with light interaction also offers the qubits, −1, 0 and 1 (Fig. 8) and this can become important to both classical and quantum computing.

Preprints (www.preprints.org) | NOT PEER-REVIEWED | Posted: 13 October 2022 doi:10.20944/preprints202210.0172.v2

⇒ **Dirac field.** Lorentz transformation of the electron to the fermion field of spin ±1/2 is applicable to the MP model (Fig. 1a). These are denoted $\psi(\mathbf{x})$ in 3D space and $\psi(\mathbf{x},t)$ in both Euclidean and Minkowski space-times (Fig. 1a and b) inclusive of the Higgs sector (Fig. 7b). The Dirac equation for the fermion field is given by,

$$i\hbar\gamma^u\partial_u\psi(x) - mc\psi(x) = 0, \tag{13}$$

where γ^u are the gamma matrices related to the shifts in the electron position of time reversal due to gravity (Fig. 1b). The exponentials of the matrices, $\{\gamma^o\gamma^1\gamma^2\gamma^3\}$ are assigned to positions, 0, 1, 2 and 3 (Fig. 1a). γ^orelates to arrow of time in asymmetry at position, 0 for a monopole field and $\gamma^1\gamma^2\gamma^3$ variables to positions, 1, 2, 3 in 3D space. These are all incorporated into the famous Dirac equation,

$$\left(i\gamma^0\frac{\partial}{\partial t} + cA\frac{\partial}{\partial x} + cB\frac{\partial}{\partial y} + cC\frac{\partial}{\partial z} - \frac{mc^2}{\hbar}\right)\psi(t,\vec{x}), \tag{14}$$

where the lightspeed, c acts on the coefficients A, B and C and transforms them to γ^1, γ^2 and γ^3. Alternatively, the exponentials of γ are denoted i, where γ^i is off-diagonal Pauli matrices at γ^1 and γ^3 with respect to the pair of light-cones (Fig. 1b). This is defined by,

$$\gamma^i = \begin{pmatrix} 0 & \sigma^i \\ -\sigma^i & 0 \end{pmatrix}, \tag{15a}$$

Preprints (www.preprints.org) | NOT PEER-REVIEWED | Posted: 13 October 2022 doi:10.20944/preprints202210.0172.v2

and zero exponential, γ^o to,

$$\gamma^0 = \begin{pmatrix} 0 & 1 \\ 1 & 0 \end{pmatrix}. \tag{15b}$$

σ^i is applicable to intersections of the BOs along the electron path for the anticommutation relationship, $e^+(\psi) \neq e^-(\bar{\psi})$ of the Lie algebra group (Fig. 4d and 7b). The matrices, 0 and 1 of Equation 15b can also relate well to Fig. 8.

⇒ **Weyl spinor.** The Weyl spinor of the pair of light-cones is applicable to the precessing MP field at the four positions, 0 to 3 (Fig. 1a). This is represented as,

$$\psi = \begin{pmatrix} \psi_0 \\ \psi_1 \\ \psi_2 \\ \psi_3 \end{pmatrix}, \tag{16}$$

and they correspond to spin up fermion, a spin down fermion, a spin up antifermion and a spin down antifermion. At 360° rotation, a spin down fermion and its antifermion is assumed. The spin up fermion and its antifermion is restored at 720° rotation (e.g., Fig. 1a). By relativistic transformation, observation is reduced to a bispinor (e.g., Fig. 5),

$$\psi = \begin{pmatrix} u_+ \\ u_- \end{pmatrix}, \tag{17}$$

where $u_\pm$ are the Weyl spinors of chiral form related to ψ_1 and ψ_3 by vertical projection along the *z*-axis (e.g., Fig. 4a). These are irreducible within the model. Parity operation *x*

Preprints (www.preprints.org) | NOT PEER-REVIEWED | Posted: 13 October 2022 doi:10.20944/preprints202210.0172.v2

$\rightarrow x' = (t, -\mathbf{x})$ for qubit 1 and −1 (Fig. 8) along the vertical axis exchanges the left- and right-handed Weyl spinor in the process,

$$\begin{pmatrix}\psi_L'\\ \psi_R'\end{pmatrix} = \begin{pmatrix}\psi_R(x)\\ \psi_L(x)\end{pmatrix} \Rightarrow \begin{matrix}\psi'(x') = \gamma^0\psi(x)\\ \bar{\psi}'(x') = \bar{\psi}(x)\gamma^0.\end{matrix} \quad (18)$$

Both left-handed (*L*) and right-handed (*R*) helicities are described in Fig. 8 with respect to 720° rotation of the electron. The Weyl spinors are converted to Dirac bispinor, $\xi^1\ \xi^2$ diagonally at positions 1 and 3 (Fig. 1a; *Postulate 4*). Normalization of the two-component spinor, $\xi^1\ \xi^2 = 1$ ensues by the orthogonal relationship, $\begin{pmatrix}1\\0\end{pmatrix}$ and $\begin{pmatrix}0\\1\end{pmatrix}$ for the full rotation of the sphere (Fig. 8). As mentioned earlier, the Lorentz transformation of matter to antimatter for the Dirac four-component spinor is comparable to Majorana fermions. However, these are constrained by observations to spin, ± 1/2 of linear time (e.g., Fig. 4a and 5). Whether their interactions with external light causes perturbations of the degenerate BOs to oscillation modes of neutrino types is open to further discussions, for these would also acquire mass in a similar process.

⇒ **Lorentz transformation.** The Hermitian, $\psi^\dagger\psi$ for the Dirac fermion transiting at positions, 0, 1, 2 and 3 (Fig. 1) is not Lorentz invariant for measurement of 1D space. These states are in superposition and offer a level of indeterminacy (Fig. 5). Weyl spinor of a light-cone depicts the relationship,

$$u^\dagger u = (\xi^\dagger\sqrt{p.\sigma},\ \xi\sqrt{p.\bar{\sigma}}\,.\begin{pmatrix}\sqrt{p.\sigma}\xi\\ \sqrt{p.\bar{\sigma}}\xi\end{pmatrix},$$

Preprints (www.preprints.org) | NOT PEER-REVIEWED | Posted: 13 October 2022 doi:10.20944/preprints202210.0172.v2

$$= 2E_P \xi^{\dagger} \xi \,. \tag{19}$$

Equation 19 would relate to 180° spherical rotation and its observation along the *z*-axis (e.g., Fig. 4a). The corresponding Lorentz scalar of the BOs is,

$$\bar{u}(p) = u^{\dagger}(p)\gamma^0, \tag{20}$$

and is referenced to time axis of the MP field. By identical calculation to Equation 19, the Weyl spinor becomes,

$$\bar{u}u = 2m\xi^{\dagger}\xi, \tag{21}$$

for the complete rotation of the sphere at 360° (Fig. 8). Based on the model, it is difficult to distinguish both Weyl spinor and Majorana fermion from the Dirac spinor by relativistic transformation (see also subsection 4.2.1).

⇒ **Quantized Hamiltonian.** The 4-vector spinors of Dirac field, $\psi(x)$ offers a level of complexity to observations (Fig. 1a). Only two ansatzes to Equation 13 are adapted as follow,

$$\psi = u(\mathbf{p})e^{-ip.x}, \tag{22a}$$

$$\psi = v(\mathbf{p})e^{ip.x}. \tag{22b}$$

Preprints (www.preprints.org) | NOT PEER-REVIEWED | Posted: 13 October 2022 doi:10.20944/preprints202210.0172.v2

These are Hermitian plane wave solutions and they form the basis for Fourier components in 3D space (e.g., Fig. 4a). Decomposition by Hamiltonian then assumes the relationships,

$$\psi(x) = \frac{1}{(2\pi)^{3/2}} \int \frac{d^3}{2E_{\mathbf{p}}} \sum_s \left(a_{\mathbf{P}}^s u^s(p) e^{-ip.x} + b_{\mathbf{P}}^{s\dagger} v^s(p) e^{ip.x} \right), \tag{23a}$$

$$\bar{\psi}(x) = \frac{1}{(2\pi)^{3/2}} \int \frac{d^3}{2E_{\mathbf{p}}} \sum_s \left(a_{\mathbf{P}}^{s\dagger} \bar{u}^s(p) e^{ip.x} + b_{\mathbf{P}}^s \bar{v}^s(p) e^{-ip.x} \right). \tag{23b}$$

The coefficients $a_{\mathbf{P}}^s$ and $a_{\mathbf{P}}^{s\dagger}$ are ladder operators, which are applicable to the BOs into *n*-dimensions along the orbital paths (e.g., Fig. 4b and d). These are for *u*-type particles and similar process is accorded to $b_{\mathbf{P}}^s$ and $b_{\mathbf{P}}^{s\dagger}$ of *v*-type particles. With unitarity sustained, Hilbert space of the model (Fig. 1b) can undergo both contraction and relaxation with external light interactions, where both types of particles are incorporated. For example, the former is accorded to Einsteinian gravity of time reversal with respect to the center and the latter to overall precession of the MP model of a clock face. The terms, $u^s(p)$ and $v^s(p)$ are Dirac spinors for the two spin states, ±1/2 and $\bar{v}^s$ and $\bar{u}^s$ for their antiparticles. The conjugate momentum is,

$$\pi = \frac{\partial \mathcal{L}}{\partial \psi} - \bar{\psi} i \gamma^0 = i \psi^\dagger. \tag{24}$$

Preprints (www.preprints.org) | NOT PEER-REVIEWED | Posted: 13 October 2022 doi:10.20944/preprints202210.0172.v2

Equation 24 is assumed by the electron in orbit of 3D space against precessing MP field of a clock face in 4D space-time (Fig. 1b). The generated oscillations are of Lagrangian mechanics (e.g., Fig. 7b) and its Hamiltonian in 3D space is,

$$H = \int d^3x\psi^\dagger(x)[-i\gamma^0\gamma.\boldsymbol{\nabla} + m\gamma^0]\,\psi(x). \tag{25}$$

The quantity in the bracket is the Dirac Hamiltonian of one-particle quantum mechanics as also shown in Equation 3. With *z*-axis aligned to time axis in asymmetry for a monopole field of a hemisphere (Fig. 4a), the currents are projected in either *x* or *y* directions in 3D space by the relationships,

$$\left[\psi_\alpha(\mathbf{x},t),\psi_\beta(\mathbf{y},t)\right] = \left[\psi_\alpha^\dagger(\mathbf{x},t),\psi_\beta^\dagger(\mathbf{y},t)\right] = 0, \tag{26a}$$

$$\left[\psi_\alpha(\mathbf{x},t),\psi_\beta^\dagger(\mathbf{y},t)\right] = \delta_{\alpha\beta}\delta^3(\mathbf{x}-\mathbf{y}), \tag{26b}$$

where α and β denote the spinor components of the ψ. Both Equations 26a and b are applicable to the Dirac fermion, whereas the Higgs sector at γ^0 or position 0 (Fig. 7b) is not influenced by the Pauli matrices including the generated $W^{\pm}$ and Z° bosons. The ψ independent of time in 3D space obeys the uncertainty principle with respect to position, **p** and momentum, **q**, as conjugate operators (Fig. 2). Their commutation relationship is,

$$\left\{a_{\mathbf{p}}^r, a_{\mathbf{q}}^{s\dagger}\right\} = \left\{b_{\mathbf{p}}^r, b_{\mathbf{q}}^{s\dagger}\right\} = (2\pi)^3\delta^{rs}\delta^3(\mathbf{p}-\mathbf{q}). \tag{27}$$

Preprints (www.preprints.org) | NOT PEER-REVIEWED | Posted: 13 October 2022 doi:10.20944/preprints202210.0172.v2

Antimatter, $b_{\mathbf{p}}^{r}, b_{\mathbf{q}}^{s\dagger}$ is produced by 360° rotation of the fermion (*Postulate 4*), whereas in practice, it is simulated by classical spin of time reversal mode. With time invariant for measurements conducted into forward time, a positive-frequency is obtained as follows,

$$\langle 0|\psi(x)\bar{\psi}(y)|0\rangle = \langle 0\,| \int \frac{d^3p}{(2\pi)^3}\frac{1}{\sqrt{2E_{\mathrm{p}}}}\sum_{r} a_{\mathrm{p}}^{r}u^{r}(p)e^{-ipx} \times \int \frac{d^3q}{(2\pi)^3}\frac{1}{\sqrt{2E_{\mathrm{q}}}}\sum_{s} a_{\mathrm{q}}^{s\dagger}\bar{u}^{s}(q)e^{iqy}\;|\,0\rangle. \tag{28}$$

Equation 28 is restricted to the BOs along *z* direction by normalizing the spin angular component in the *x* and *y* directions (e.g., Fig. 4a). In this way, Dirac strings are constrained by the dipole moments of the MP field.

⇒ **Further undertakings.** The above interpretations with respect to the Dirac fermion demonstrate the compatibility of the model to QFT application as an approximate intuitive guide to the quantum state. Other related themes that can perhaps be explored in a similar manner include Fock space and Fermi-Dirac statistics, Bose-Einstein statistics, causality, Feynman propagator, charge conjugation, parity, charge-parity-time symmetry and so forth. In this case, the boundary posed by the model could justify the removal of infinities during renormalization process such as for the perturbation theory to conform to measurements.

Preprints (www.preprints.org) | NOT PEER-REVIEWED | Posted: 13 October 2022 doi:10.20944/preprints202210.0172.v2

5. Conclusion

The intuitive form of the Dirac fermion unveiled within the applied MP model has far reaching implications. It is able to incorporate both relativistic and non-relativistic wave function comparable to the application of QFTs. The outcomes are shown to pave the path for a quantum universe, where the Lagrangian terms of the SM and Einstein field equations are incorporated into a geometric space-time of the model. This assumes a multiverse of the models at a hierarchy of energy scales. Though the approach remains somewhat highly speculative to some extent, it offers new insights into phenomena like the hierarchy problem, monopoles existence, baryon asymmetry and so forth. If considered, this could pave the paths for the pursuits of physics from a different perspective altogether beyond the Standard Model by conventional methods and it warrants further investigations.

Competing financial interests

The author declares no competing financial interests.

 doi:10.20944/preprints202210.0172.v2

References

1. E. Nelson. Derivation of the Schrödinger equation from Newtonian mechanics. *Phys. Rev.* 150(4), 1079 (1966).
2. C. Rovelli. Space is blue and birds fly through it. *Philos. Trans. Royal Soc. Proc. Math. Phys. Eng.* 376(2123), 20170312 (2018).
3. D. H. Perkins. Proton decay experiments. *Ann. Rev. Nucl. Part. Sci.* 34(1), 1-50 (1984).
4. H. Sun. Solutions of nonrelativistic Schrödinger equation from relativistic Klein–Gordon equation. *Phys. Lett. A* 374(2), 116-122 (2009).
5. S. Oshima, S. Kanemaki & T. Fujita. Problems of Real Scalar Klein-Gordon Field. *arXiv preprint hep-th/0512156* (2005).
6. S. D. Bass, A. De Roeck & M. Kado. The Higgs boson implications and prospects for future discoveries. *Nat. Rev. Phys.* 3(9), 608-624 (2001).
7. S. P. Yuguru. Unconventional reconciliation path for quantum mechanics and general relativity. *IET Quant. Comm.* 3(2), 99–111 (2022). https://doi.org/10.1049/qtc2.12034
8. L. S. Weiss et al. Controlled creation of a singular spinor vortex by circumventing the Dirac belt trick. *Nat. Commun.* 10(1), 1-8 (2019).
9. Z. K. Silagadze. Mirror objects in the solar system?. *arXiv preprint astro-ph/0110161* (2001).
10. G. F. Giudice. The dawn of the post-naturalness era. *arXiv preprint arXiv:*1710.07663 (2017).
11. P. Atkins & J. de Paula. *Physical Chemistry*. 9th Edition. Oxford University Press, New York (2010).

12. https://chem.libretexts.org/Courses/Pacific_Union_College/Quantum_Chemistry/10%3A_Bonding_in_Polyatomic_Molecules/10.04%3A_Photoelectron_Spectroscopy
13. A. Szabo & N. S. Ostlund. *Modern quantum chemistry: introduction to advanced electronic structure theory*. Courier Corporation, Massachusetts, USA (1996).
14. H. Haken & H. C. Wolf. *The physics of atoms and quanta: introduction to experiments and theory* (Vol. 1439, No. 2674). Springer Science & Business Media (2005).
15. G. Gabrielse et al. New determination of the fine structure constant from the electron g value and QED. *Phys. Rev. Lett.* 97(3), 030802 (2006).
16. D. Hanneke et al. Cavity control of a single-electron quantum cyclotron: Measuring the electron magnetic moment. *Phys. Rev. A* 83(5), 052122 (2011).
17. D. J. Gross. Nobel lecture: The discovery of asymptotic freedom and the emergence of QCD. *Rev. Mod. Phys.* 77(3), 837 (2005).
18. S. Weinberg. Implications of dynamical symmetry breaking. *Phys. Rev. D* 13, 974 (1976).
19. N. Craig. Naturalness hits a snag with Higgs. *Physics* 13, 174 (2020).
20. N. Arkani-Hamed & S. Dimopoulos. Supersymmetric unification without low energy supersymmetry and signatures for fine-tuning at the LHC. *J. High Energy Phys.* 2005(06), 073 (2005).
21. K. Benakli et al. A fake split-supersymmetry model for the 126 GeV Higgs. *J. High Energy Phys.* 2014 (5), 1-23 (2014).
22. H. Baer et al. Multichannel assault on natural supersymmetry at the high luminosity LHC. *Phys. Rev. D* 94(3), 035025 (2016).

23. G. S. Guralnik et al. Broken symmetries and the Goldstone theorem. *Adv. Part. Phys.* 2, 567-708 (1968).

24. J. Woithe et al. Let's have a coffee with the standard model of particle physics!. *Phys. Educ.* 52(3), 034001 (2017).

25. F. J. Huang, Q. H. Chen & W. M. Liu. Higgs-like Excitations of Cold Atom System with Spin-orbit Coupling. *arXiv preprint arXiv:1207.3707* (2012).

26. C. W. Misner, K. S. Thorne & W. H. Zurek. John Wheeler, relativity, and quantum information. *Phys. Today* 62(4), 40-46 (2009).

27. M. W. Evans et al. Criticisms of the Einstein Field Equation (Vol. 3). Cambridge International Science Publishing (2011).

28. B. P. Abbott et al. GW150914: Implications for the stochastic gravitational-wave background from binary black holes. *Phys. Rev. Lett.* 116(13), 131102 (2016).

29. M. E. Peskin & D. V. Schroeder. *An introduction to quantum field theory*. Addison-Wesley, Massachusetts, USA (1995).

30. L. Alvarez-Gaumé & M. A. Vazquez-Mozo. Introductory lectures on quantum field theory. *arXiv preprint hep-th/0510040* (2005).

31. G. Eichmann. Lectures on Quantization of the Dirac Field (2020) http://cftp.ist.utl.pt/%7Egernot.eichmann/lecture-notes